

Synthesis, Structure, and Reactivity of Diazoketiminato Complexes of Platinum(II) and Palladium(II): Cytotoxic Properties of a Platinum Complex

Jahar Lal Pratihar,^[a] Biswaranjan Shee,^[a] Poulami Pattanayak,^[a] Debprasad Patra,^[a] Arindam Bhattacharyya,^[b] Vedavati G. Puranik,^[c] C. H. Hung,^[d] and Surajit Chattopadhyay*^[a]

Keywords: Chelating ligands / Platinum / Palladium / Redox chemistry / Bioinorganic chemistry

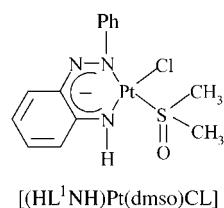
Reaction of the 2-(aryloxy)anilines $\text{Ar-N=N-C}_6\text{H}_4\text{NH}_2$ [HL^nNH_2 ; Ar = C_6H_5 (HL^1), $p\text{-CH}_3\text{C}_6\text{H}_4$ (HL^2), $p\text{-ClC}_6\text{H}_4$ (HL^3)] with K_2PtCl_4 in dmsO affords the new Pt^{II} azoimine complexes $[(\text{HL}^n\text{NH})\text{Pt}(\text{dmsO})\text{Cl}]$ where the chloride and dmsO ligands are mutually *cis*. In contrast, treatment of Na_2PdCl_4 with HL^nNH_2 in dmsO gives the chloro-bridged palladium dimer $[(\text{HL}^n\text{NH})\text{PdCl}]_2$ as the major product along with $[(\text{HL}^n\text{NH})_2\text{Pd}]$ as the minor product. Further, the reaction of $\text{HL}^n\text{NHCH}_2\text{Ph}$ with K_2PtCl_4 in dmsO also gives $[(\text{HL}^n\text{NH})\text{Pt}(\text{dmsO})\text{Cl}]$ whereas Na_2PdCl_4 affords the ortho-palladated complexes $[(\text{L}^n\text{NHCH}_2\text{Ph})\text{PdCl}]$. This means that the $\text{N-C}(\text{CH}_2\text{Ph})$ bond is selectively cleaved by K_2PtCl_4 . The reaction of $[(\text{HL}^n\text{NH})\text{Pt}(\text{dmsO})\text{Cl}]$ with acetylacetone (acacH)

gives the heteroleptic complex $[(\text{HL}^n\text{NH})\text{Pt}(\text{acac})]$. $[(\text{HL}^n\text{NH})\text{Pt}(\text{dmsO})\text{Cl}]$ and $[(\text{HL}^n\text{NH})\text{Pt}(\text{acac})]$ display a reversible reductive response at -1.20 and -1.46 V vs. SCE, respectively, in their cyclic voltammograms. The nature of the redox orbitals has been determined semi-empirically employing the EHMO method. The cytotoxicity of $[(\text{HL}^1\text{NH})\text{Pt}(\text{dmsO})\text{Cl}]$ has been examined with HeLa cells and the sub-lethal dose ($8 \mu\text{M}$) determined by dose-dependence studies. The relative degree of apoptotic and necrotic cell death using a sub-lethal dose were measured by flow cytometry.

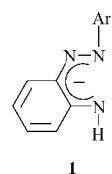
© Wiley-VCH Verlag GmbH & Co. KGaA, 69451 Weinheim, Germany, 2007

Introduction

Pt^{II} complexes have been known for a long time and their importance was enhanced with the discovery of cisplatin. Cisplatin and carboplatin are two widely used anticancer drugs although there are certain limitations in their therapeutic uses, therefore several appropriately designed models of Pt^{II} complexes have been clinically tested in search of suitable alternatives.^[1–9] One of the proposed models for Pt^{II} -based chemotherapeutic agents is $[\text{Pt}(\text{L})(\text{dmsO})\text{Cl}]$, where L is a bidentate anionic ligand and the anticipated labile ligands are dimethyl sulfoxide (dmsO) and chloride.^[10–13] These reports encouraged us to study the *in vitro* cytotoxic properties of our newly synthesized diazoketiminato complex $[(\text{HL}^1\text{NH})\text{Pt}(\text{dmsO})\text{Cl}]$ in view of its importance as a potential model of anticancer agents.



The work reported here stems from our interest in the coordination chemistry of platinum complexes incorporating bidentate (N,N), anionic, and delocalized diazoketimine ligands **1**. We have previously reported the bis-chelate complexes of Pd^{II} and Pt^{II} incorporating **1**,^[14,15] and herein we report the reactions of Na_2PdCl_4 and K_2PtCl_4 with the ligand precursors $\text{Ar-N=N-C}_6\text{H}_4\text{NH}_2$ [HL^nNH_2 ; Ar = C_6H_5 (HL^1), $p\text{-CH}_3\text{C}_6\text{H}_4$ (HL^2), $p\text{-ClC}_6\text{H}_4$ (HL^3)] and $\text{HL}^n\text{NHCH}_2\text{Ph}$ in dmsO. Aspects related to $\text{N-C}(\text{alkyl})$ bond cleavage with K_2PtCl_4 , the redox properties of the new platinum complexes formed, and a comparison of the reactivities of Pt^{II} and Pd^{II} substrates toward similar ligands are also described in this paper.



[a] Department of Chemistry, University of Kalyani, Kalyani 741235, India
E-mail: schas8@rediffmail.com

[b] Department of Environmental Science, University of Kalyani, Kalyani 741235, India

[c] Center for Materials Characterization, National Chemical Laboratory, Pune 411008, India

[d] National Changhua University of Education, Changhua 50058, Taiwan

Supporting information for this article is available on the WWW under <http://www.eurjic.org> or from the author.

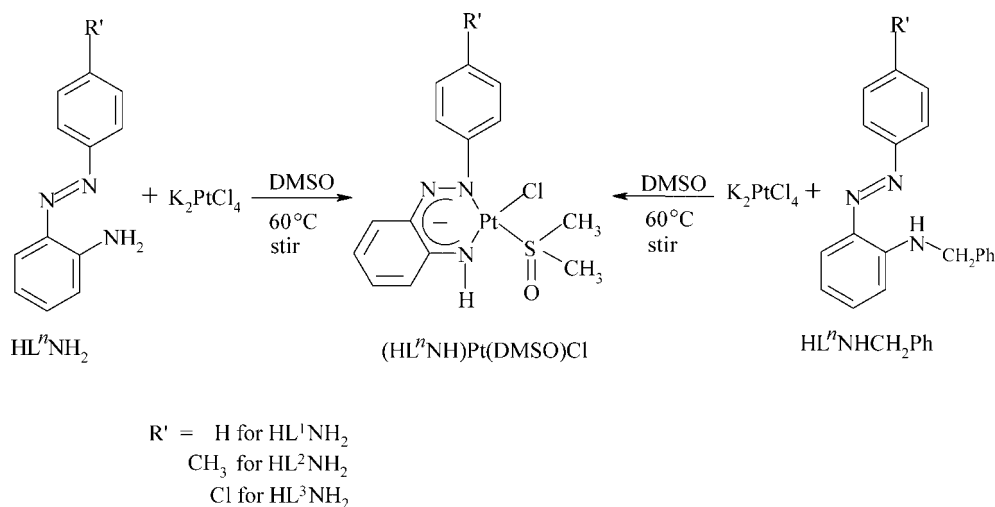
Reaction of the 2-(arylo)anilines HL^nNH_2 or their *N*-benzylated derivative HL^nNHCH_2Ph with K_2PtCl_4 affords the electroactive complexes of the desired composition, namely $[(HL^nNH)Pt(dmsO)Cl]$. Reaction of the same ligands with Na_2PdCl_4 was also performed to confirm that cleavage of the *N*-C(benzyl) bond only occurs with K_2PtCl_4 . The reactions of $[(HL^nNH)Pt(dmsO)Cl]$ with the bidentate ligand *acacH* to give the new heteroleptic bis complexes of composition $[(HL^nNH)Pt(acac)]$ show the feasibility of substituting the Cl^- and *dmsO* ligands in this complex. All new complexes have been characterized unequivocally and their structures confirmed by X-ray crystallography. The electron-transfer properties of the Pt^{II} com-

plexes have been examined electrochemically and the results rationalized by employing semi-empirical EHMO calculations. The dose dependence and nature of cell (HeLa) death (apoptotic or necrotic) have also been studied for $[Pt(HL^1NH)(dmsO)Cl]$.

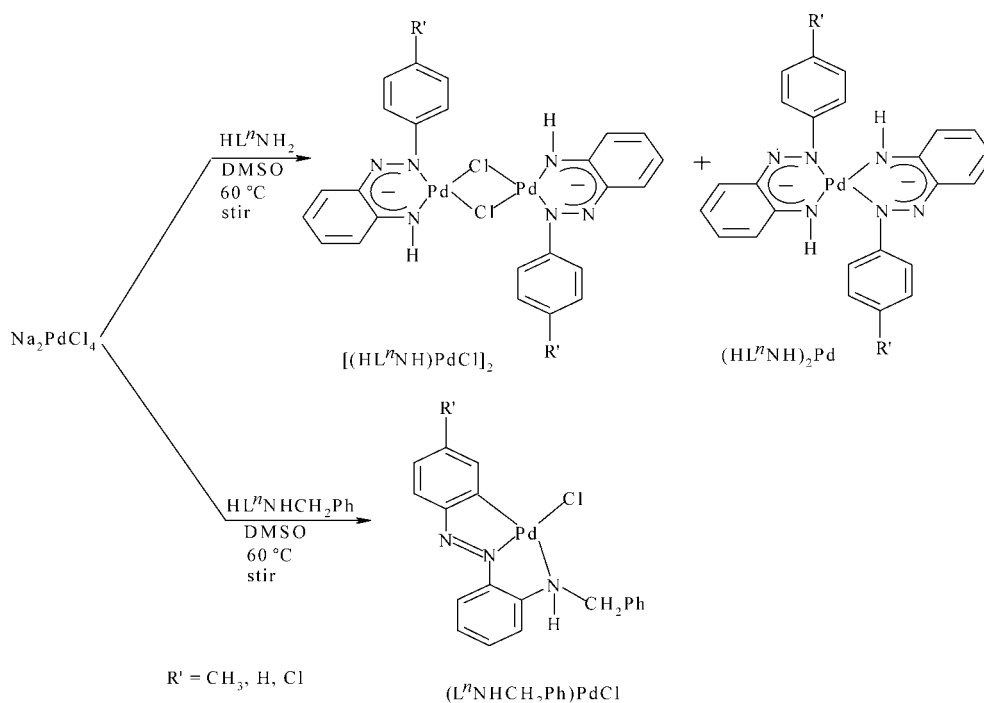
Results and Discussion

Syntheses and Reactions

The reaction of HL^nNH_2 or HL^nNHCH_2Ph with K_2PtCl_4 in warm *dmsO* affords the pink complexes $[(HL^nNH)Pt(dmsO)Cl]$ in good yield (Scheme 1). Addition



Scheme 1.



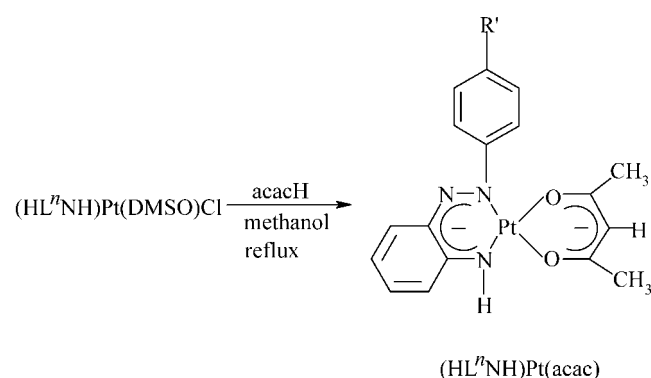
Scheme 2.

of K_2PtCl_4 to warm dmsO is expected to form the dmsO-coordinated Pt^{II} complex, which is likely to be the actual metal substrate that reacts with the ligands.

The formation of $[(HL^nNH)Pt(dmsO)Cl]$ prompted us to examine the reactions of the same ligands with Na_2PdCl_4 in warm dmsO. The results of these reactions are summarized in Scheme 2.

The minor product $[Pd(HL^nNH)_2]$ has been prepared in good yield previously,^[14] while the major product, $\{[(HL^nNH)PdCl]_2\}$, is isolated here for the first time. Its structure was confirmed by X-ray crystallography (see below). The orthopalladated complex $[(L^nNHCH_2Ph)PdCl]$ was obtained, as expected,^[16] upon treatment of HL^nNHCH_2Ph with Na_2PdCl_4 , whereas the same reaction with K_2PtCl_4 gives $[(HL^nNH)Pt(dmsO)Cl]$ by cleavage of the N–C(benzyl) bond of HL^nNHCH_2Ph . Subtle difference in the properties of Pt^{II} and Pd^{II} are likely to be the origin of this mismatch in reactivity between Na_2PdCl_4 and K_2PtCl_4 .

Reaction of $[(HL^nNH)Pt(dmsO)Cl]$ with the bidentate ligand acetylacetonone (acacH) was performed in boiling methanol to give the blue neutral heteroleptic bis complex $[(HL^nNH)Pt(acac)]$ (Scheme 3). Substitution of the mutu-



Scheme 3.

ally *cis* dmsO and Cl^- ligands of $[(HL^nNH)Pt(dmsO)Cl]$ by acetylacetonate indicates the possibility of coordination of this complex with the nucleoside bases of nucleic acids.

Spectroscopic Characterization

The complexes $[(HL^nNH)Pt(dmsO)Cl]$ and $[(HL^nNH)Pt(acac)]$ dissolve in common organic solvents to give pink and blue solutions, respectively, consistent with the relative energies of absorptions in the visible region {approx. 560 nm for $[(HL^nNH)Pt(dmsO)Cl]$ and approx. 600 nm for $[(HL^nNH)Pt(acac)]$ }. The positions of other higher energy absorption bands for all the complexes are alike with characteristic shifts. The relevant data are collected in Table 1 and representative spectra of $[(HL^1NH)Pt(dmsO)Cl]$ and $[(HL^1NH)Pt(acac)]$ are shown in Figure 1.

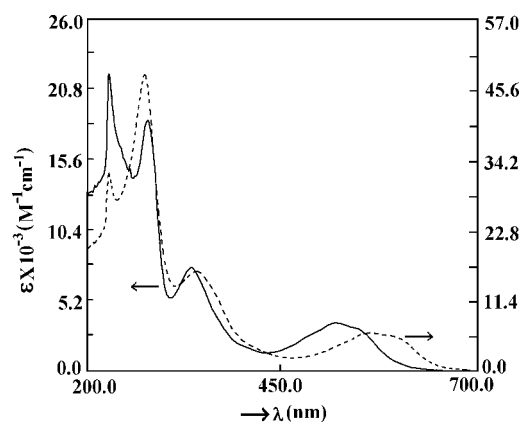


Figure 1. UV/Vis spectra of $[(HL^1NH)Pt(dmsO)Cl]$ (—) and $[(HL^1NH)Pt(acac)]$ (---). The arrows indicate the scales of the corresponding spectrum.

The IR spectra of complexes $[(HL^nNH)Pt(dmsO)Cl]$ in solid KBr exhibit sharp ν_{N-H} absorptions in the range 3284–3291 cm^{-1} , thereby indicating the presence of one

Table 1. UV/Vis,^[a] IR,^[b] and cyclic voltammetric data for $[(HL^nNH)Pt(dmsO)Cl]$, $[(HL^nNH)Pt(acac)]$, and $\{[(HL^1NH)PdCl]_2\}$.

Compound	λ_{max} [nm] (ϵ [$M^{-1} cm^{-1}$])	$\tilde{\nu}$ [cm^{-1}]					$E_{1/2}$ [V] ^[c] (ΔE_p [mV])
		ν_{N-H}	$\nu_{C=N}$	$\nu_{N=N}$	$\nu_{S=O}$	ν_{Pt-Cl}	
$[(HL^1NH)Pt(dmsO)Cl]$	555 (7300), 520 (8640) 330 (18400), 280 (44660)	3284	1618	1341	1112	371	−1.120 (80)
$[(HL^2NH)Pt(dmsO)Cl]$	560 (5180), 530 (5890) 340 (14500), 275 (34600)	3291	1615	1342	1118	374	−1.246 (95)
$[(HL^3NH)Pt(dmsO)Cl]$	560 (11320), 530 (12270) 3400 (27350), 275 (71130)	3289	1617	1342	1120	372	−1.152 (95)
$[(HL^1NH)Pt(acac)]$	600 (7430), 565 (6600) 340 (17150), 270 (51230)	3330	1615	1341	—	—	−1.473 (110)
$[(HL^2NH)Pt(acac)]$	600 (2800), 565 (3070) 350 (10800), 270 (25870)	3321	1616	1347	—	—	−1.510 (115)
$[(HL^3NH)Pt(acac)]$	600 (4800), 570 (5420) 345 (14120), 270 (37850)	3320	1617	1340	—	—	−1.410 (100)
$\{[(HL^1NH)PdCl]_2\}$	560 (5000), 525 (5150) 330 (17100)	3338	1615	1333	—	—	—

[a] In dichloromethane. [b] In KBr disc. [c] vs. SCE in CH_3CN as solvent; supporting electrolyte: NBu_4ClO_4 .

amino proton. Surprisingly, the complexes $[(HL^nNH)Pt(acac)]$ exhibit two overlapping ν_{N-H} absorptions in the range $3320\text{--}3350\text{ cm}^{-1}$, which may be due to a site effect in the solid state.^[17] The $\nu_{N=N}$ absorptions of both complexes are shifted to lower frequency ($1340\text{--}1347\text{ cm}^{-1}$) than in the free ligands HL^nNH_2 (approx. 1460 cm^{-1}).^[14,15,18,19] The strong band observed at around 1617 cm^{-1} which is absent in the free ligands can be assigned to the $\nu_{C=N}$ absorption.^[14,15,18,19] The blue-shift of the $\nu_{S=O}$ absorption for complexes $[(HL^nNH)Pt(dmsO)Cl]$ ($1112\text{--}1120\text{ cm}^{-1}$) compared to free dmsO (1050 cm^{-1}) indicates S-coordination. The ν_{Pt-Cl} absorption of $[(HL^nNH)Pt(dmsO)Cl]$ appears in the range $371\text{--}374\text{ cm}^{-1}$. Relevant IR data are also collected in Table 1.

The 1H NMR spectra of complexes $[(HL^nNH)Pt(dmsO)Cl]$ display a resonance near $\delta = 3.5$ ppm for coordinated dmsO while the aromatic protons of the coordinated $(HL^nNH)^-$ ligands appear in the range $\delta = 6.58\text{--}7.75$ ppm. The proton counts match well with the composition, thereby indicating no mismatch with the molecular structure in solution. The 1H NMR spectroscopic data are listed in Table 2. Although the spectrum of $[(HL^nNH)Pt(dmsO)Cl]$ is slightly more complicated in the aromatic region, the proton count is consistent with the composition. The spectra of $[(HL^2NH)Pt(dmsO)Cl]$ and $[(HL^3NH)Pt(dmsO)Cl]$ are well resolved in the aromatic region, where two doublets and two triplets, each integrating for one proton, appear for 2-H, 3-H, 4-H, and 5-H (the atom numbering scheme is shown in Figure 3, a). Two doublets, each integrating for two equivalent protons, are observed for 8,12-H and 9,11-H. A representative spectrum for $[(HL^2NH)Pt(dmsO)Cl]$ is shown in Figure 2. The N–H resonances for these complexes fall within the aromatic region and are overlapped by other resonances of the aromatic protons. However, the proton count matches the composition $(HL^nNH)^-$, thereby confirming the removal of one NH_2 proton upon complexation.

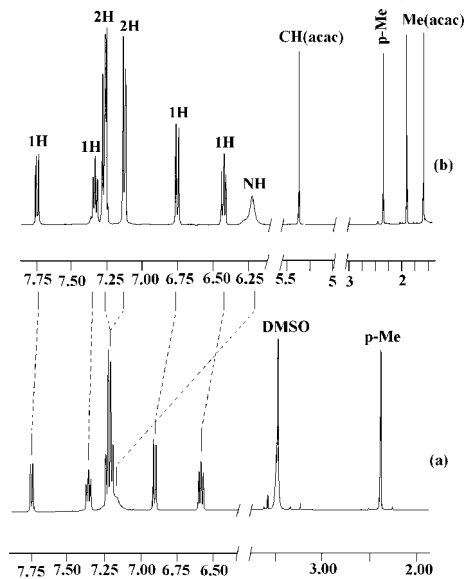


Figure 2. Correlation of aromatic proton resonances along with the proton count of $[(HL^2NH)Pt(dmsO)Cl]$ (a) and $[(HL^2NH)Pt(acac)]$ (b).

The 1H NMR spectra of the $[(HL^nNH)Pt(acac)]$ complexes exhibit the N–H resonance as a broad singlet in the range $\delta = 6.22\text{--}6.35$ ppm, thereby confirming the $(HL^nNH_2) \rightarrow (HL^nNH)^-$ transformation. The 1H NMR spectra of $[(HL^nNH)Pt(acac)]$ are similar to those of $[(HL^nNH)Pt(dmsO)Cl]$ in the aromatic region but with slightly different chemical shift values. A one-to-one correlation of the aromatic protons is shown in Figure 2 for $[(HL^2NH_2)Pt(acac)]$ and $[(HL^2NH)Pt(dmsO)Cl]$. The coordinated acac ligand of $[(HL^nNH)Pt(acac)]$ shows three sets of resonances, one for the methine proton ($\delta \approx 5.35$ ppm) and two for the CH_3 groups ($\delta \approx 1.92$ and 1.59 ppm),

Table 2. 1H NMR spectroscopic data for $[(HL^nNH)Pt(dmsO)Cl]$, $[(HL^nNH)Pt(acac)]$, and $[\{(HL^1NH)PdCl\}_2]$.

Compound	δ [ppm] ^[a] Aromatic H	Nonaromatic H	R (CH_3)	N–H
$[(HL^1NH)Pt(dmsO)Cl]$	7.75 (d, 1 H), 7.40 (t, 2 H), 7.38–7.25 (m, 4 H) 6.90 (d, 1 H), 6.59 (t, 1 H)	3.50 (s, 6 H)	–	7.17 (br., 1 H)
$[(HL^2NH)Pt(dmsO)Cl]$	7.74 (d, 1 H), 7.35 (t, 1 H), 7.24–7.18 (m, 4 H) 6.90 (d, 1 H), 6.58 (t, 1 H)	3.50 (s, 6 H)	2.40 (s, 3 H)	7.17 (br., 1 H)
$[(HL^3NH)Pt(dmsO)Cl]$	7.71 (d, 1 H), 7.38–7.34 (m, 3 H), 7.28 (d, 2 H) 6.90 (d, 1 H), 6.60 (t, 1 H)	3.51 (s, 6 H)	–	–
$[(HL^1NH)Pt(acac)]$	7.74 (d, 1 H), 7.38 (d, 2 H), 7.36–7.32 (m, 3 H) 7.27 (d, 1 H), 6.76 (d, 1 H), 6.43 (t, 1 H)	5.36 (s, 1 H), 1.92 (s, 3 H) 1.56 (s, 3 H)	–	6.28 (br., 1 H)
$[(HL^2NH)Pt(acac)]$	7.74 (d, 1 H), 7.38 (t, 1 H), 7.28–7.24 (m, 2 H) 7.13 (d, 2 H), 6.75 (d, 1 H), 6.42 (t, 1 H)	5.37 (s, 1 H), 1.92 (s, 3 H) 1.58 (s, 3 H)	2.37 (s, 3 H)	6.22 (br., 1 H)
$[(HL^3NH)Pt(acac)]$	7.72 (d, 1 H), 7.36–7.30 (m, 5 H), 6.75 (d, 1 H) 6.44 (t, 1 H)	5.39 (s, 1 H), 1.93 (s, 3 H) 1.63 (s, 3 H)	–	6.35 (br., 1 H)
$[\{(HL^1NH)PdCl\}_2]$	8.08–8.00 (m, 1 H), 7.85 (t, 1 H), 7.57–7.36 (m, 2 H), 7.19 (t, 1 H), 6.88 (d, 1 H), 6.74–6.51 (m, 3 H)	–	–	4.91 (br., 1 H)

[a] In $CDCl_3$.

thereby indicating an unequal chemical environment about the two Me groups, consistent with the X-ray structure (see below).

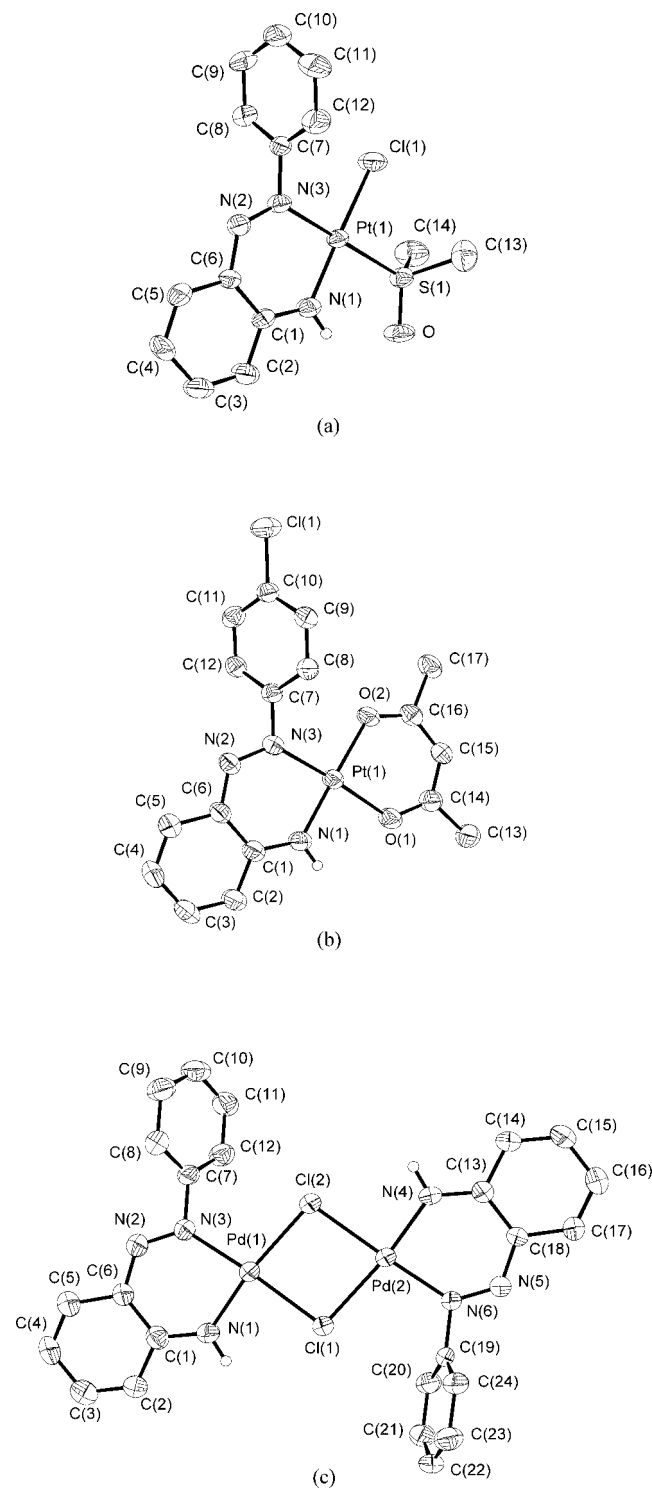


Figure 3. Perspective views of $[(HL^1NH)Pt(dmsO)Cl]$ (a), $[(HL^3NH)Pt(acac)]$ (b), and $\{[(HL^1NH)PdCl]_2\}$ (c) with atom numbering scheme. Hydrogen atoms, except those on N1 in (a), (b), and (c) and N4 in (c), have been omitted for clarity.

X-ray Structures

The crystal structures of $[(HL^1NH)Pt(dmsO)Cl]$, $\{[(HL^1NH)PdCl]_2\}$, and $[(HL^3NH)Pt(acac)]$ were determined as representative examples of each type of complex. The (HL^nNH) ligands bind to the metals in an N,N-bidentate fashion in all three complexes. A chloride and a dmsO ligand (coordinated to the Pt^{II} through its S atom) are present in the coordination sphere of $[(HL^1NH)Pt(dmsO)Cl]$, and the acac⁻ ligand of $[(HL^3NH)Pt(acac)]$ binds Pt^{II} in an O,O-bidentate fashion as expected. Two bridging chloride

Table 3. Selected bond lengths [Å] and angles [°] for $[(HL^1NH)Pt(dmsO)Cl]$, $[(HL^3NH)Pt(acac)]$, and $\{[(HL^1NH)PdCl]_2\}$.

$[(HL^1NH)Pt(dmsO)Cl]$			
Pt(1)–Cl(1)	2.320(2)	N(1)–C(1)	1.317(6)
Pt(1)–S(1)	2.241(2)	N(2)–N(3)	1.282(5)
Pt(1)–N(1)	1.957(4)	N(2)–C(6)	1.353(6)
Pt(1)–N(3)	2.026(4)	N(3)–C(7)	1.465(6)
S(1)–O	1.466(4)	C(1)–C(6)	1.445(6)
S(1)–C(13)	1.779(5)	S(1)–C(14)	1.775(5)
Cl(1)–Pt(1)–S(1)	87.94(4)	C(13)–S(1)–C(14)	101.5(2)
Cl(1)–Pt(1)–N(1)	176.44(10)	O–S(1)–C(14)	108.2(2)
Cl(1)–Pt(1)–N(3)	93.66(11)	Pt(1)–N(1)–C(1)	129.0(3)
S(1)–Pt(1)–N(1)	89.50(10)	N(3)–N(2)–C(6)	123.4(4)
S(1)–Pt(1)–N(3)	175.30(9)	Pt(1)–N(3)–C(7)	120.2(3)
N(1)–Pt(1)–N(3)	89.08(14)	N(2)–N(3)–C(7)	110.7(3)
Pt(1)–S(1)–O	115.05(15)	O–S(1)–C(13)	109.5(2)
Pt(1)–S(1)–C(13)	108.42(15)	Pt(1)–S(1)–C(14)	113.32(15)
$[(HL^3NH)Pt(acac)]$			
Pt(1)–O(1)	2.026(3)	N(2)–N(3)	1.303(4)
Pt(1)–O(2)	2.031(3)	N(2)–C(6)	1.356(6)
Pt(1)–N(1)	1.940(4)	N(3)–C(7)	1.439(6)
Pt(1)–N(3)	1.975(4)	C(1)–C(6)	1.431(8)
O(1)–C(14)	1.273(6)	C(14)–C(15)	1.385(7)
O(2)–C(16)	1.278(6)	C(15)–C(16)	1.409(8)
N(1)–C(1)	1.327(6)		
O(1)–Pt(1)–O(2)	93.41(12)	N(2)–C(6)–C(1)	128.4(4)
Pt(1)–O(2)–C(16)	122.5(3)	O(1)–Pt(1)–N(1)	84.49(14)
O(1)–Pt(1)–N(3)	175.19(13)	Pt(1)–N(1)–C(1)	128.7(4)
O(2)–Pt(1)–N(3)	91.28(13)	O(2)–Pt(1)–N(1)	177.02(15)
N(1)–Pt(1)–N(3)	90.87(15)	C(14)–C(15)–C(16)	127.3(5)
Pt(1)–O(1)–C(14)	123.6(3)	Pt(1)–N(3)–C(7)	122.1(3)
O(1)–C(14)–C(15)	126.2(5)	N(3)–N(2)–C(6)	123.0(4)
N(2)–C(6)–C(5)	113.3(5)	N(2)–N(3)–C(7)	109.8(4)
Pt(1)–N(3)–N(2)	128.1(3)		
$\{[(HL^1NH)PdCl]_2\}$			
Pd(1)–Cl(1)	2.3596(11)	C(5)–C(6)	1.425(5)
Pd(1)–Cl(2)	2.3678(11)	C(4)–C(5)	1.333(7)
Pd(1)–N(1)	1.938(3)	C(3)–C(4)	1.411(7)
Pd(1)–N(3)	2.004(3)	C(2)–C(3)	1.343(6)
N(1)–C(1)	1.315(5)	C(1)–C(2)	1.425(6)
N(2)–N(3)	1.281(5)	N(3)–C(7)	1.448(6)
N(2)–C(6)	1.339(5)	C(1)–C(6)	1.430(6)
Cl(2)–Pd(1)–N(3)	98.61(10)	N(1)–C(1)–C(2)	119.7(4)
Cl(2)–Pd(1)–N(1)	172.14(10)	C(2)–C(1)–C(6)	118.0(3)
Cl(1)–Pd(1)–N(3)	175.96(10)	N(1)–C(1)–C(6)	122.3(4)
Cl(1)–Pd(1)–N(1)	87.45(10)	N(2)–C(6)–C(5)	115.9(4)
N(2)–C(6)–C(1)	126.3(3)	Cl(1)–Pd(1)–Cl(2)	84.71(4)
N(2)–N(3)–C(7)	112.2(3)	Pd(1)–N(3)–C(7)	119.7(3)
Pd(1)–N(1)–C(1)	129.1(3)	Pd(1)–N(3)–N(2)	128.1(3)
N(1)–Pd(1)–N(3)	89.20(14)	N(3)–N(2)–C(6)	124.5(3)
C(3)–C(4)–C(5)	119.5(4)	C(1)–C(6)–C(5)	117.7(4)
C(1)–C(2)–C(3)	121.0(4)		

ligands coordinate the Pd^{II} apart from the bidentate (HL¹NH)⁻ ligand in [(HL¹NH)PtCl]₂. The (HL¹NH)⁻ ligands in this molecule are mutually *trans* with no substantial mismatch in the bond parameters. Perspective views of the molecules are shown in Figures 3 (a–c), and selected bond lengths and angles are collected in Table 3.

The geometries about the metal center are planar (mean deviations within 0.0216–0.0532 Å) for all three neutral molecules, thereby confirming the bivalent state of Pt and Pd and the formation of a mononegative anionic ligand (HLⁿNH)⁻ by dissociation of an amine proton from the precursor HLⁿNH₂, consistent with the IR and ¹H NMR spectroscopic data (see above).^[14,15,18,19] The equality in bond lengths within the chelate ring framework of coordinated acetylacetonate of [(HLⁿNH)Pt(acac)] signifies the expected delocalization upon deprotonation.^[20] The C(1)–N(1) distances (approx. 1.324 Å) of all three molecules are much shorter than that of the C(7)–N(3) single bond (approx. 1.444 Å) in the same molecules. The C(1)–N(1) distances are, in fact, similar to that of an imine (approx. 1.34 Å).^[14,15,18,19] The effect of delocalization within the chelate framework of (HLⁿNH)⁻ is further reflected by the adjacent phenyl ring [C(1)–C(6)], which has four long and two short bonds. The C(6)–N(2) bond length (approx. 1.35 Å) is shorter than the C(7)–N(3) single bond length as a consequence. These structural features allowed us to infer the formation of delocalized diazoketiminato chelates.^[14,15,18,19]

The asymmetric unit of [(HLⁿNH)Pt(acac)] contains two mutually *trans* molecules that are held together by a weak Pt^{II}...Pt^{II} interaction (3.898 Å). The stacking arrangement displayed by this weak dimer in the crystal lattice is shown in Figure 4 (inter dimer Pt^{II}...Pt^{II} distance is 4.320 Å). The Pd^{II}...Pd^{II} distance in the [(HLⁿNH)PdCl]₂ dimer is 3.494 Å, which means that there is no Pd–Pd single bond formation and no possibility of forming a Pd^I–Pd^I dimer.

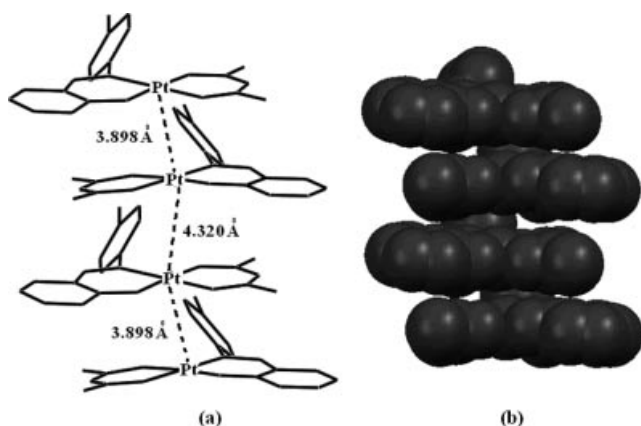


Figure 4. (a) Partial packing diagram and (b) stacking arrangement of [(HL³NH)Pt(acac)].

Electrochemistry

The cyclic voltammograms of complexes [(HLⁿNH)Pt(dmsO)Cl] display a quasi-reversible one-electron re-

duction (calibrated against the current height of the Fc/Fc⁺ couple) in the range $E_{1/2} \approx -1.120$ to -1.246 V vs. SCE in acetonitrile. The voltammogram of [(HL¹NH)Pt(dmsO)Cl] is shown in Figure 5 (a) as an example. The overall redox reactions are represented in Equation (1). The $E_{1/2}$ values vary systematically with R' of the (HLⁿNH) ligand, and a plot of $E_{1/2}$ vs. σ (the Hammett substituent constant) is linear (Figure 5, b).^[21]

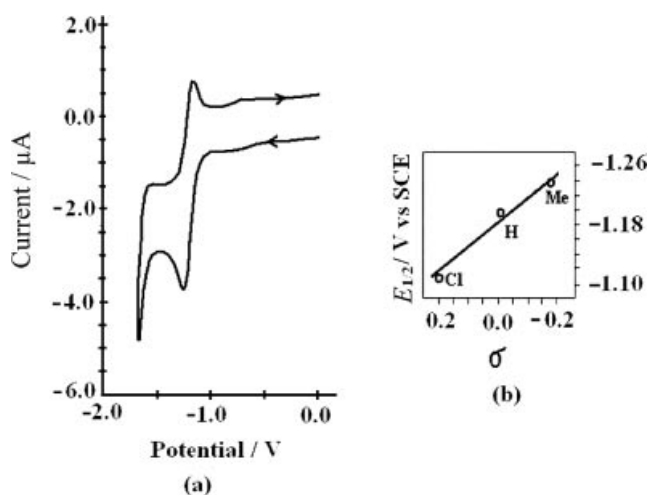
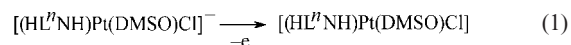


Figure 5. (a) Cyclic voltammogram of [(HL¹NH)Pt(dmsO)Cl] in acetonitrile solution (0.1 M NBu₄ClO₄) vs. SCE. (b) A least-squares plot of $E_{1/2}$ values of [(HLⁿNH)Pt(dmsO)Cl] complexes vs. σ (Hammett substituent constant).

To gain an insight into the nature of the redox orbitals we performed EHMO calculations^[22,23] using the crystallographic atomic coordinates of [(HL¹NH)Pt(dmsO)Cl]. The energy level and interaction diagram was determined by FMO analysis, which showed that the LUMO is a non-bonding ligand group orbital (Figure 6). The contribution of an antibonding group combination of azo (–N=N–) nitrogens to the LUMO is 50%, therefore the reductive response of [(HLⁿNH)Pt(dmsO)Cl] may be assigned to reduction of the azo function [Equation (2)].^[24,25] The cyclic voltammogram of [(HLⁿNH)Pt(acac)] is similar (see Figure S16) to that of the [(HLⁿNH)Pt(dmsO)Cl] complexes but with a characteristic shift of the $E_{1/2}$ values (-1.410 V to -1.510 V vs. SCE in acetonitrile). An EHMO calculation was also performed with the crystallographic atomic coordinates of [(HL³NH)Pt(acac)], and analysis of the LUMO showed a similar composition to that of [(HLⁿNH)Pt(dmsO)Cl], with a contribution from the azo- π^* combination of also about 50%. The energy-level diagram with metal–ligand interactions and the orbital diagram of LUMO are given in Figure S1 (see Supporting Information).



Cytotoxicity

HeLa cells were treated with [(HL¹NH)Pt(dmsO)Cl] in the concentration range 4.0–20.0 μ M. A viability plot of the

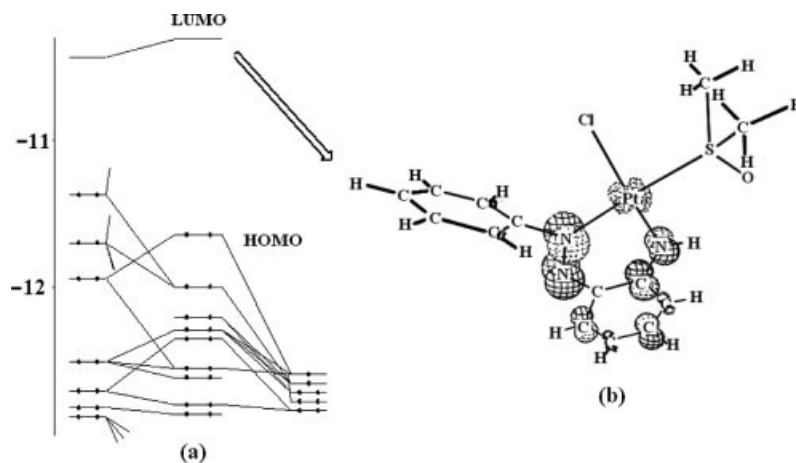


Figure 6. (a) Partial energy level and interaction diagram and (b) MO drawing of the LUMO of $[(HL^1NH)Pt(dmsO)Cl]$.

trypan blue dye exclusion assay is shown in Figure 7. The trypan blue assay showed that ED_{75} , which is the effective dose of $[(HL^1NH)Pt(dmsO)Cl]$ required to kill 75% of cells, is $12 \mu M$ for this complex. Around 50% of the cells were still viable after 5 h from the time of treatment of the cells with $8 \mu M$ $[(HL^1NH)Pt(dmsO)Cl]$, which is therefore the sub-lethal dose.^[26] The pattern of cell death was studied by flow cytometric technique using appropriate dye stains. The apoptotic cell death was studied by the Annexin-V binding assay technique using a sub-lethal dose ($8 \mu M$) of $[(HL^1NH)Pt(dmsO)Cl]$. The cells were co-stained with propidium iodide (PI) in addition to Annexin V to distinguish between apoptotic and necrotic cell death.^[27] Although the later stages of apoptosis cannot be distinguished from necrosis, the flipped-out phosphatidylserine residue selectively binds Annexin V-FITC on the cells' surface during the early stages of apoptosis. The results of the flow cytometric measurements are shown in Figure 8. Viable cells are negative to both dyes (PI and Annexin V-FITC), as shown in the bottom-left quadrant of Figure 8. The Annexin V conjugated cells appearing in the bottom-right quadrant of Fig-

ure 8 represent the apoptotic cells, and the upper-right quadrant represents the Annexin V and PI conjugated cells, which indicates late-stage apoptosis or necrosis.

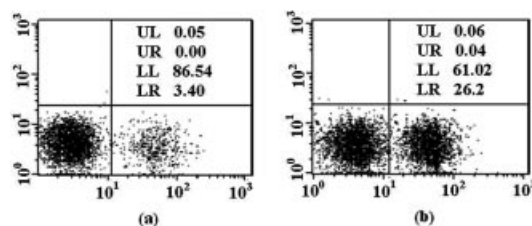


Figure 8. Flow cytometric measurements with HeLa cells using Annexin V-FITC/PI to distinguish between apoptosis and necrosis: (a) the plot for untreated cells; (b) the plot for cells treated with $[(HL^1NH)Pt(dmsO)Cl]$. UL = upper left, UR = upper right, LL = lower left, LR = lower right.

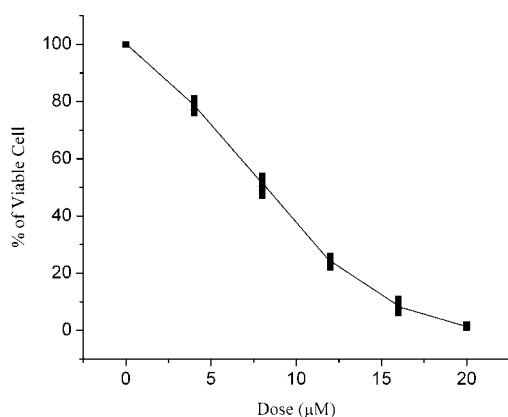


Figure 7. Plot of dose vs. viable cells to determine the sub-lethal dose.

These studies show the cytotoxic effects of this new class of platinum(II) chelate complexes $[(HL^1NH)Pt(dmsO)Cl]$ with mutually *cis*-coordinated dmsO and chloride ligands. Although activation of apoptosis is a remarkable observation, a comparison of the results obtained with cisplatin is necessary and is currently underway.

Concluding Remarks

The reactions of K_2PtCl_4 with HL^nNH_2 and HL^nNHCH_2Ph in refluxing dmsO both afford the diazoketiminato complex $[(HL^nNH)Pt(dmsO)Cl]$ due to N–C(benzyl) bond cleavage in HL^nNHCH_2Ph . In contrast, Na_2PdCl_4 affords the orthopalladated complexes and chloro-bridged diazoketiminatodipalladium complexes upon reaction with HL^nNHCH_2Ph and HL^nNH_2 , respectively. The reaction of $[(HL^nNH)Pt(dmsO)Cl]$ with acacH affords the new heteroleptic complex $[(HL^nNH)Pt(acac)]$, thereby indicating the possibility of binding bioligands by substituting the chloride and/or dmsO ligands of $[(HL^nNH)Pt(dmsO)Cl]$. The crystal structure of $[(HL^nNH)Pt(acac)]$ exhibits a stacked

arrangement with weak intermolecular interactions. Interestingly, the delocalized diazoketiminato chelates [(HLⁿNH)-Pt(dmsO)Cl] and [(HLⁿNH)Pt(acac)] exhibit reversible one-electron reductions in their cyclic voltammograms. This electron-transfer property has been attributed to a ligand-centered reversible azo (–N=N–) reduction by EHMO calculations. The results of an in vitro study of the cytotoxicity of [(HL¹NH)Pt(dmsO)Cl] against the HeLa cell line are interesting in terms of dose dependence and apoptotic pattern of cell death. Further biological experiments are underway to compare the relative activities with cisplatin.

Experimental Section

Materials: The solvents used in the reactions were of reagent grade (E. Merck, Kolkata, India) and were purified and dried by reported procedures.^[14] Platinum chloride, dimethyl sulfoxide, and acetylacetone were purchased from the same company. Potassium tetrachloroplatinate and sodium tetrachloropalladate were prepared by a reported procedure. Trypan blue, propidium iodide, and Annexin V-FITC were obtained from Aldrich. HeLa cells were collected from NCCS, Pune, India. The ligands 2-(phenylazo)aniline (HL¹NH₂), 2-(*p*-tolylazo)aniline (HL²NH₂), and 2-(*p*-chlorophenylazo)aniline (HL³NH₂) were prepared following the reported procedures.^[14,15,18]

Physical Measurements: Microanalysis (C,H,N) was performed using a Perkin–Elmer 240C elemental analyzer. Infrared spectra were recorded with a Perkin–Elmer L120-00A FT-IR spectrometer with the samples prepared as KBr pellets. Electronic spectra were recorded with a Shimadzu UV-2401 PC spectrophotometer. ¹H NMR spectra were obtained with Bruker 500 RPX and Bruker 300 DPX spectrometers in CDCl₃ using TMS as the internal standard. Electrochemical measurements were performed using a PAR Versastat II potentiostat with a platinum disk working electrode, a platinum wire auxiliary electrode, and an aqueous saturated calomel electrode (SCE) as reference, (0.1 M) Bu₄NClO₄ as supporting electrolyte, in acetonitrile. Electrochemical measurements were carried out under a dinitrogen atmosphere at 298 K and were uncorrected for junction potentials. Cytotoxicity was measured with a Fluorescence Microscope (Olympus BX40, Tokyo, Japan), FACS Calibur (BD Biosciences) and the Cell Quest (Bekton Dickinson) software package.

Synthesis of [(HL¹NH)Pt(dmsO)Cl]: A solution of 2-(phenylazo)aniline (HL¹NH₂; 100 mg, 0.5 mmol) in 5 mL of dmsO was added to a solution of K₂PtCl₄ (207 mg, 0.5 mmol) in 5 mL of the same solvent. The mixture was stirred for 5 h at 60 °C and a dark pink solid was obtained upon evaporation of dmsO. Pure [(HL¹NH)Pt(dmsO)Cl] was obtained from the pink solid by chromatography on a silica gel (60–120 mesh) column with toluene as the eluent. Solid [(HL¹NH)Pt(dmsO)Cl] was obtained by evaporating the eluent. Yield: 115.25 mg (45%). C₁₄H₁₆ClN₃OPtS (504.9): calcd. C 33.25, H 3.18, N 8.34; found C 33.27, H 3.16, N 8.31.

[(HL²NH)Pt(dmsO)Cl] and [(HL³NH)Pt(dmsO)Cl]: These complexes were prepared following the same procedure as for [(HL¹NH)Pt(dmsO)Cl] but with HL²NH₂ (106 mg, 0.5 mmol) and HL³NH₂ (116 mg, 0.5 mmol). Yield: 104.27 mg (40%, for the HL²NH₂ complex C₁₅H₁₈ClN₃OPtS) and 121.62 mg (45%, for the HL³NH₂ complex C₁₄H₁₅Cl₂N₃OPtS). C₁₅H₁₈ClN₃OPtS (518.9): calcd. C 34.71, H 3.41, N 8.12; found C 34.68, H 3.46, N 8.09. C₁₄H₁₅Cl₂N₃OPtS (539.4): calcd. C 31.10, H 2.80, N 7.82; found C 31.14, H 2.78, N 7.78.

[(HL¹NH)Pt(acac)]: [(HL¹NH)Pt(dmsO)Cl] (50 mg, 0.1 mmol) was dissolved in 40 mL of methanol and acetylacetone (10 mg, 0.38 mmol) was added. The mixture was then heated to reflux for 4 h to afford a blue solution. Evaporation of the solvent gave a dark blue residue, which was purified by chromatography on a silica gel (60–120 mesh) column with toluene as eluent. Evaporation of the solvent gave [(HL¹NH)Pt(acac)] as a dark blue solid. Yield: 32.10 mg (65%). C₁₇H₁₇N₃O₂Pt (490.36): calcd. C 41.55, H 3.48, N 8.53; found C 41.60, H 3.46, N 8.56.

[(HL²NH)Pt(acac)] and [(HL³NH)Pt(acac)]: These compounds were prepared following the same procedure as for [(HL¹NH)Pt(acac)] but with [(HL²NH)Pt(dmsO)Cl] (52 mg, 0.1 mmol) and [(HL³NH)Pt(dmsO)Cl] (54 mg, 0.1 mmol). Yield: 35.05 mg (70%, for the HL²NH complex C₁₈H₁₉N₃O₂Pt) and 36.24 mg (70%, for the HL³NH complex C₁₇H₁₆ClN₃O₂Pt). C₁₈H₁₉N₃O₂Pt (504.36): calcd. C 42.85, H 3.79, N 8.29; found C 42.82, H 3.76, N 8.32. C₁₇H₁₆ClN₃O₂Pt (524.86): calcd. C 38.83, H 3.08, N 8.05; found C 38.86, H 3.04, N 8.00.

[(HL¹NH)PdCl₂]: A solution of HL¹NH₂ (100 mg, 0.5 mmol) in 5 mL of dmsO was added to a solution of Na₂PdCl₄ (150 mg, 0.5 mmol) in 5 mL of dmsO. The mixture was stirred for 4 h at 60 °C and a dark pink solid was obtained upon evaporation of dmsO. Pure [(HL¹NH)PdCl₂] was obtained from the pink solid by chromatography on a silica gel (60–120 mesh) column with toluene as the eluent. Solid [(HL¹NH)PdCl₂] was obtained upon evaporation of the eluent. Yield: 188.80 mg (55%). C₂₄H₂₀Cl₂N₆Pd₂ (1352.5): calcd. C 42.59, H 2.95, N 12.42; found C 42.54, H 3.01, N 12.38.

Reaction of HL¹NHCH₂Ph with Na₂PdCl₄: A solution of HL¹NHCH₂Ph (110 mg, 0.52 mmol) in 5 mL of dmsO was added to a solution of Na₂PdCl₄ (150 mg, 0.52 mmol) in 5 mL of dmsO. The mixture was stirred for 4 h at 60 °C and a dark brown solid was obtained upon evaporation of dmsO. Pure [(HL¹NHCH₂Ph)PdCl] was obtained from the brown solid by chromatography on a silica gel (60–120 mesh) column with a toluene/acetonitrile mixture (90:10 v/v) as eluent. Solid [(L¹NHCH₂Ph)PdCl] was obtained upon evaporation of the eluent. Yield: 119.99 (55%).

Reaction of HL¹NHCH₂Ph with K₂PtCl₄: A solution of HL¹NHCH₂Ph (110 mg, 0.52 mmol) in 5 mL of dmsO was added to a solution of K₂PtCl₄ (215 mg, 0.52 mmol) in 5 mL of dmsO. The mixture was stirred for 5 h at 60 °C and a dark pink solid was obtained upon evaporation of dmsO. Pure [(HL¹NH)Pt(dmsO)Cl] was isolated by chromatography on a silica gel (60–120 mesh) column with toluene as the eluent. Solid [(HL¹NH)Pt(dmsO)Cl] was obtained upon evaporation of the eluent. Yield: 130.76 mg (50%).

Viability Assay. Trypan Blue Exclusion Test: HeLa cells were treated with 4, 8, 12, and 16 μM solutions of complex in dmsO.^[28] The cells (10 μL suspension) were then placed on cover slips at the required dilution and each cover slip was placed cell-side down onto a slide containing a drop of 0.125% Trypan Blue dye (wt/vol in sterile isotonic saline). The excess dye solution was removed by applying gentle pressure with gauze at the edges of the cover slip. The slides were viewed within ten minutes with a light microscope at a magnification of 40× and 50–100 cells counted. Viable cells remained unstained, while the nuclei of nonviable cells were stained blue.

Differentiation Between Apoptosis and Necrosis by FACS: To distinguish between apoptosis and necrosis treated or untreated cells (1 × 10⁶ in each case) were harvested, in a double labeling system, and PI and Annexin V Fluos (Boehringer Mannheim) added directly to the culture medium or to the cell suspension. The mixture

Table 4. Crystallographic data for [(HL¹NH)Pt(dmsO)Cl], [(HL³NH)Pt(acac)], and [{(HL¹NH)PdCl}₂].

	[(HL ¹ H)Pt(dmsO)Cl]	[(HL ³ NH)Pt(acac)]	[(HL ¹ NH)PdCl] ₂
Formula	C ₁₄ H ₁₆ ClN ₃ O ₂ PtS	C ₁₇ H ₁₆ ClN ₃ O ₂ Pt	C ₂₄ H ₂₀ Cl ₂ N ₆ Pd ₂
<i>M</i>	504.90	524.86	1352.4
Space group	<i>Fdd2</i>	<i>P</i> $\bar{1}$	<i>P</i> $\bar{1}$
Crystal system	orthorhombic	triclinic	triclinic
<i>a</i> [Å]	21.573(18)	8.185(3)	10.3262(10)
<i>b</i> [Å]	30.81(2)	13.720(5)	10.3626(10)
<i>c</i> [Å]	9.838(7)	16.257(6)	12.2239(12)
α [°]	90	107.007(9)	101.710(2)
β [°]	90	90.176(9)	112.079(2)
γ [°]	90	91.980(10)	92.665(2)
λ [Å]	0.71073	0.71073	0.71073
<i>V</i> [Å ³]	6539(8)	1744.6(11)	1176.0(2)
<i>Z</i>	16	4	2
<i>D</i> _{calcd.} [g cm ⁻³]	2.051	1.998	1.910
μ [mm ⁻¹]	8.875	8.210	1.783
<i>R</i> ₁ ^[a]	0.0184	0.0322	0.0309
<i>wR</i> ₂ ^[b]	0.0340	0.0701	0.0648
Unique reflections [<i>I</i> > 2 σ (<i>I</i>)	21173/3886	28481/9547	7504/5218
GOF ^[c]	0.81	1.000	0.96

[a] $R_1 = \sum ||F_o| - |F_c|| / \sum |F_o|$. [b] $wR_2 = \sum [w(F_o^2 - F_c^2)^2] / \sum [w(F_o^2)^2]^{1/2}$ where $w = 1/\sigma^2(F_o^2) + (aP)^2 + bP$, $P = (F_o^2 + 2F_c^2)/3$. [c] GOF = $\sum [w(F_o^2 - F_c^2)^2] / (n - p)$.

was then incubated for 15 min at 37 °C. Excess PI and Annexin V Fluos were washed off, and the cells were fixed and then analyzed with a FACS Calibur apparatus [equipped with a 488-nm argon laser light source, a 515-nm band pass filter (FL1-H), and a 623-nm band pass filter (FL2-H)] using the CellQuest program (Becton Dickinson). Electronic compensation of the instrument was done to exclude overlapping of the emission spectra. A total of 10,000 events were acquired, the cells were properly gated, and a dual parameter dot plot of FL1-H (*x*-axis; Fluos fluorescence) vs. FL2-H (*y*-axis; PI fluorescence) was produced in logarithmic fluorescence intensity.^[29]

X-ray Crystallography: Crystals of [(HL¹NH)Pt(dmsO)Cl], [(HL³NH)Pt(acac)], and [{(HL¹NH)PdCl}₂] were grown by diffusion of hexane into a dichloromethane solution at 298 K. Data were collected with a Bruker SMART CCD diffractometer using Mo-*K*_α-monochromated radiation ($\lambda = 0.71043$ Å). Structure solutions were performed using the Shelx 97 program (PC version). Full-matrix least-squares and anisotropic refinements were performed on all the atoms. Hydrogen atoms were included at their calculated positions. The data collection parameters and relevant crystal data are collected in Table 4.

CCDC-283817 for [(HL¹NH)Pt(dmsO)Cl], -283818 for [(HL³NH)Pt(acac)], and -283819 for [{(HL¹NH)PdCl}₂] contain the supplementary crystallographic data for this paper. These data can be obtained free of charge from The Cambridge Crystallographic Data Centre via www.ccdc.cam.ac.uk/data_request/cif.

Supporting Information (see also the footnote on the first page of this article): Figure S1 shows the EHMO diagrams for [(HL³NH)Pt(acac)]. Figures S2–S8 show the IR spectra and Figures S9–S15 the ¹H NMR spectra of all the complexes; Figure S16 shows the cyclic voltammogram of [(HL¹NH)Pt(acac)].

Acknowledgments

We are thankful to the Department of Science and Technology (DST), New Delhi for funding and a fellowship to J. P. under the DST-SERC project (no. SR/S1/IC-09/2003). We are also thankful to the Council of Scientific and Industrial Research for funding.

The necessary laboratory and infrastructural facilities were provided by the Department of Chemistry, University of Kalyani. The support of DST under the FIST program to the Department of Chemistry, University of Kalyani is acknowledged. We acknowledge Prof. Jui-Hsien Huang, National Changhua University of Education, Changhua, Taiwan for performing the X-ray studies of [(HL³NH)Pt(acac)].

- [1] B. Rosenberg, L. V. Camp, *Nature* **1965**, *205*, 698–699.
- [2] B. Rosenberg, L. V. Camp, J. E. Trosko, V. H. Mansour, *Nature* **1969**, *222*, 385–386.
- [3] B. Rosenberg, L. V. Camp, *Cancer Res.* **1970**, *30*, 1799–1802.
- [4] R. B. Weiss, M. C. Christian, *Drugs* **1993**, *46*, 360–377.
- [5] J. Reedijk, *Inorg. Chim. Acta* **1992**, *198–200*, 873–881.
- [6] C. F. J. Barnard, *Platinum Met. Rev.* **1989**, *33*, 162–167.
- [7] T. W. Hambley, *Coord. Chem. Rev.* **1997**, *166*, 181–223.
- [8] G. Natile, M. Coluccia, *Coord. Chem. Rev.* **2001**, *216–217*, 383–410.
- [9] A. G. Quiroga, C. Navarro Ranninger, *Coord. Chem. Rev.* **2004**, *248*, 119–133.
- [10] C. Sacht, M. S. Datt, S. Otto, A. Rood, *J. Chem. Soc. Dalton Trans.* **2000**, 727–733.
- [11] C. Sacht, M. S. Datt, S. Otto, A. Rood, *J. Chem. Soc. Dalton Trans.* **2000**, 4579–4586.
- [12] C. Sacht, M. Datt, *Polyhedron* **2000**, *19*, 1347–1354.
- [13] A. Rodger, K. K. Patel, K. J. Sanders, M. Datt, C. Sacht, M. J. Hannon, *J. Chem. Soc. Dalton Trans.* **2002**, 3656–3663.
- [14] N. Maiti, S. Pal, S. Chattopadhyay, *Inorg. Chem.* **2001**, *40*, 2204–2205 and references cited therein.
- [15] N. Maiti, S. Chattopadhyay, *Indian. J. Chem. Sect. A* **2003**, *42*, 2327–2331.
- [16] J. Pratihari, N. Maiti, P. Pattanayak, S. Chattopadhyay, *Polyhedron* **2005**, *24*, 1953–1960.
- [17] J. Pratihari, N. Maiti, S. Chattopadhyay, *Inorg. Chem.* **2005**, *44*, 6111–6114.
- [18] N. Maiti, B. K. Dirghangi, S. Chattopadhyay, *Polyhedron* **2003**, *22*, 3109–3113.
- [19] J. Pratihari, D. Patra, S. Chattopadhyay, *J. Organomet. Chem.* **2005**, *690*, 4816–4821.
- [20] M. Ghedini, D. Pucci, A. Crispini, G. Barberio, *Organometallics* **1999**, *18*, 2116–2124.
- [21] L. P. Hammett, *Physical Organic Chemistry*, 2nd edn., McGraw Hill, New York, **1970**.

- [22] C. Mealli, D. M. Proserpio, *CACAO* Version 4.0, Italy, **1994**.
- [23] C. Mealli, D. M. Proserpio, *J. Chem. Educ.* **1990**, *67*, 399–403.
- [24] P. K. Santra, D. Das, T. K. Misra, R. Roy, C. Sinha, S.-M. Peng, *Polyhedron* **1999**, *18*, 1909–1915.
- [25] T. K. Misra, D. Das, C. Sinha, P. Ghosh, C. K. Pal, *Inorg. Chem.* **1998**, *37*, 1672–1678.
- [26] L. Axanova, D. J. Morré, D. M. Morré, *Cancer Lett.* **2005**, *225*, 35–40.
- [27] H. Ashush, L. A. Rozenszajn, M. Blass, M. Barda-Saad, D. Azimov, J. Radnay, D. Zipori, U. Rosenschein, *Cancer Res.* **2000**, *60*, 1014–1020.
- [28] C. Gaiddon, P. Jeannequin, P. Bischoff, M. Pfeffer, C. Sirlin, J. P. Loeffler, *J. Pharmacol. Exp. Ther.* **2005**, *315*, 1403–1411.
- [29] A. Bratasz, N. M. Wei, N. L. Parinandi, J. L. Zweier, R. Sridhar, L. J. Ignarro, P. Kuppasamy, *Pharmacology* **2006**, *103*, 3914–3919.

Received: March 28, 2007

Published Online: July 31, 2007